Identification of recurrent 3q13.31 chromosomal rearrangement indicates *LSAMP* as a tumor suppressor gene in neuroblastoma

ANGELA MARTINEZ-MONLEON[1], JENNIE GAARDER[1], ANNA DJOS[1], PER KOGNER[2] and SUSANNE FRANSSON[1]

[1]Department of Laboratory Medicine, Sahlgrenska Academy at University of Gothenburg, SE-405 30 Gothenburg; [2]Childhood Cancer Research Unit, Department of Women's and Children's Health, Karolinska Institutet, SE-171 77 Stockholm, Sweden

Received November 30, 2021; Accepted November 4, 2022

DOI: 10.3892/ijo.2023.5475

Abstract. Neuroblastoma (NB) is a childhood malignancy of the sympathetic nervous system. NB is mainly driven by copy number alterations, such as *MYCN* amplification, large deletions of chromosome arm 11q and gain of chromosome arm 17q, which are all markers of high-risk disease. Genes targeted by recurrent, smaller, focal alterations include *CDKN2A/B*, *TERT*, *PTPRD* and *ATRX*. Our previous study on relapsed NB detected recurrent structural alterations centered at limbic system-associated membrane protein (*LSAMP*; HUGO Gene Nomenclature Committee: 6705; chromosomal location 3q13.31), which is a gene frequently reported to be deleted or downregulated in other types of cancer. Notably, in cancer, *LSAMP* has been shown to have tumor-suppressing functions. The present study performed an expanded investigation using whole genome sequencing of tumors from 35 patients, mainly with high-risk NB. Focal duplications or deletions targeting *LSAMP* were detected in six cases (17%), whereas single nucleotide polymorphism-microarray analysis of 16 NB cell lines detected segmental alterations at 3q13.31 in seven out of the 16 NB cell lines (44%). Furthermore, low expression of *LSAMP* in NB tumors was significantly associated with poor overall and event-free survival. *In vitro*, knockdown of *LSAMP* in NB cell lines increased cell proliferation, whereas overexpression decreased proliferation and viability. These findings supported a tumor suppressor role for *LSAMP* in NB. However, the higher incidence of *LSAMP* aberrations in cell lines and in relapsed NB tumors suggested that these alterations were a late event predominantly in advanced NB with a poor prognosis, indicating a role of *LSAMP* in tumor progression rather than in tumor initiation. In conclusion, the present study demonstrated recurrent genomic aberrations of chromosomal region 3q13.31 that targeted the *LSAMP* gene, which encodes a membrane protein involved in cell adhesion, central nervous system development and neurite outgrowth. The frequent aberrations affecting *LSAMP*, together with functional evidence, suggested an anti-proliferative role of *LSAMP* in NB.

Correspondence to: Dr Susanne Fransson, Department of Laboratory Medicine, Sahlgrenska Academy at University of Gothenburg, Medicinaregatan 3B, SE-405 30 Gothenburg, Sweden
E-mail: susanne.fransson@clingen.gu.se

Key words: neuroblastoma, tumor suppressor, genomic, genetic, cancer, Ig-like cell adhesion, limbic system-associated membrane protein

Introduction

Neuroblastoma (NB) is a pediatric neuroendocrine tumor of the sympathetic nervous system. NB arises from undifferentiated neural crest precursor cells, which results in tumors emerging mainly in the adrenal medulla or paraspinal ganglia. It is the most common malignancy diagnosed in the first year of life and the most common extracranial solid tumor in childhood (1). NB represents 8-10% of all pediatric tumors, but results in ~15% of all pediatric cancer deaths (2,3). Tumors commonly arise in children <5 years of age with an average age of 18 months at the time of diagnosis (4). Understanding NB is a challenge due to the heterogeneity in the course of the disease, ranging from tumors that show spontaneous regression (even without treatment) to highly aggressive tumors with a treatment-resistant phenotype. Patients with high-risk NB (HR-NB) have a very poor prognosis, with <50% 5-year overall survival rate despite heavy multimodal treatment, and the survival rate is <10% for relapsed cases (5). Considering the high mortality rate associated with HR-NB, increased understanding of the biology behind this malignancy is important as it may lead to improvement in patient stratification and ultimately in novel therapeutic strategies.

Analysis of chromosomal copy number variations (CNVs) in NB provides relevant information for the diagnosis and prognosis of the disease. Tumors with numerical aberrations only (gain/loss of whole chromosomes) and near triploid karyotype are typically associated with a good prognosis, whereas tumors with segmental rearrangements and near di- or tetraploid karyotypes generally have a poor prognosis (6,7). Recurrent CNVs in NB include loss of chromosome 1p, 3p, 4p and 11q, gain of 1q, 2p and 17q, and amplification of the *MYCN* oncogene; notably, *MYCN* amplification and

11q-deletion are associated with more aggressive NB. Small focal alterations have been shown to target cell cycle genes (e.g., *CDKN2A/B, CCND1, CDK4/6* and *MDM2*) (8-10) or genes involved in chromatin remodeling and telomere maintenance (e.g., *ATRX, ARID1A/ARID1B* and *TERT*) (11,12). Whereas large segmental alterations are common in NB, the somatic acquisition of small genetic alterations are relatively rare in sporadic NB, with recurrent alterations mainly found in *ALK, ATRX, PTPN11* and *TIAM1* (13-15). However, as the use of large-scale, high-throughput techniques, such as next generation sequencing, is expanding, additional recurrent aberrations that contribute to the development and progression of NB are expected to be detected (16).

Recent whole genome sequencing (WGS) studies performed by us and others have detected recurrent structural variants (SVs) that affect the limbic system-associated membrane protein (*LSAMP*) gene located in chromosomal region 3q13.31 (12,17). *LSAMP* encodes a protein member of the Ig-like cell adhesion (IgLON) family of proteins, which also include opioid-binding protein/cell adhesion molecule like (*OPCML*), neuronal growth regulator 1 (*NEGR1*), neurotrimin (*NTM*) and *IGLON5* (18). All of the IgLON members have been shown to be expressed during central nervous system development, and are involved in cell adhesion, neurite outgrowth (19), dendritic arborization, neuronal development (20) and synapse formation (21,22). Alterations in IgLONs have been reported to be associated with mental disorders (23-25) and also different types of cancer, where they function as tumor suppressor genes (26-28).

The presence of LSAMP has been observed in neural crest cells in experiments conducted in chickens (19), indicating that it may be relevant in the context of NB, as it is considered a malignancy caused by dysregulation of embryonic neural crest development (29). In addition, LSAMP is reportedly involved in axon guidance during the limbic system development (30), neurite outgrowth in dorsal root ganglia (31) and psychiatric disorders (24,32). Notably, it has also previously been reported as a tumor suppressor gene in several types of cancer (33-44).

Given that *LSAMP* has been shown to have a role in neural development and has been implicated as a tumor suppressor gene in different types of cancer, the present study hypothesized that *LSAMP* could have a tumor-suppressing capacity in NB. This was investigated in the present study by examining the frequency and extent of recurrent genomic alterations targeting the *LSAMP* gene in NB tumors and NB cell lines through WGS and single nucleotide polymorphism (SNP)-microarrays, together with *in vitro* exploration of the functional implication of *LSAMP* re-expression or silencing.

Materials and methods

Tumor material and cell lines. All NB samples from Swedish patients (n=35) were collected after obtaining written informed consent from their parents or guardians, and were analyzed according to permits approved by the Karolinska Institutet and the Karolinska University Hospital ethics committees (Stockholm, Sweden; approval no. 2009/1369-31/1) in agreement with The Declaration of Helsinki. Sampling was performed during routine clinical procedures, and treatment was performed according to established national and international protocols. Demographic and genomic data of patients are outlined in Table I. The NB cell lines NB1, NB69, SK-N-AS, SK-N-BE(2), SK-N-F1, SK-N-DZ, SK-N-SH, SH-SY5Y, KELLY and IMR-32 were obtained from the American Type Culture Collection. LS and NGP cell lines were kindly provided by Prof. Manfred Schwab (DKFZ, Heidelberg, Germany), whereas the CLB-GAR, CLB-BAR, CLB-PE and CLB-GE cell lines were retrieved from the Centre Léon Bérard (Lyon, France) under a material transfer agreement. All cell lines were cultured in high-glucose DMEM (Gibco; Thermo Fisher Scientific, Inc.) supplemented with 10% FBS (Gibco; Thermo Fisher Scientific, Inc.) at 37˚C in an atmosphere containing 5% CO_2, and were routinely verified to be negative for mycoplasma, bacterial and fungal infection.

WGS analysis. DNA from primary tumor and corresponding normal samples from 35 patients were analyzed by WGS, including seven patients from our recent study where relapsed tumor material was also subject to sequencing (12). Tumor DNA was extracted from fresh frozen tissue and constitutional DNA from the blood using DNeasy Blood and Tissue Kit (Qiagen GmbH) with sequencing, subsequent bioinformatics handling and variant filtering performed as described previously (12). Briefly, pair-end sequencing was conducted on NovaSeq 6000 (Illumina, Inc.) with an average coverage of at least 60X for tumor material and 30X for constitutional DNA. The Sentieon TNscope software version 201911 (Sentieon, Inc., Mountain View, CA) was used for mapping to hg19, removal of read duplicates, realignment around InDels and variant calling, whereas QIAGEN Clinical Insight Interpret software (version 8.1.20210827; Qiagen GmbH) was used for systematic filtering of called variants. Copy number profiles were generated using the CANVAS tool (version 1.38.0.1554) (45) and somatic SVs were called using the Manta tool (version 1.1.1) (46). All called SVs were evaluated by manual inspection using Integrative Genomics Viewer (version 2.3.81) (47).

SNP-array analysis. CytoScan™ HD-microarrays (cat. no. 901835; Applied Biosystems; Thermo Fisher Scientific, Inc.) were also used to analyze copy number changes on the tumor samples from the 35 patients with NB in combination with 16 NB cell lines [NB1, NB69, CLB-GAR, CLB-BAR, CLB-PE, CLB-GE, SK-N-AS, SK-N-BE(2), SK-N-F1, SK-N-DZ, SK-N-SH, SH-SY5Y, KELLY, IMR-32, LS and NGP] to corroborate and further explore the 3q13.31 chromosomal region. The arrays were scanned using a confocal laser scanner, GeneChip Scanner 3000 (Applied Biosystems; Thermo Fisher Scientific, Inc.) with normalization of the tumor samples performed *in silico* with genomic annotation based on the hg19 human genome. The procedure for handling CytoScan HD microarrays has been described previously (48).

Sanger sequencing analysis. Primers for *LSAMP* breakpoint verification were designed either using Primer-BLAST (https://www.ncbi.nlm.nih.gov/tools/primer-blast/) or placed manually with specificity evaluated through UCSC In-Silico PCR (https://genome.ucsc.edu/), and were used together with PLATINUM SuperFI PCR Master Mix (Thermo Fisher Scientific, Inc.) for PCR amplification, according to the manufacturer's instructions. Primer sequences are presented

Table I. Demographic and genomic features of the study cohort.

Characteristic	Whole cohort (n=35)	*LSAMP*-deleted (n=6)	*LSAMP* not deleted (n=29)
Sex			
Female	17	2	15
Male	18	4	14
Age, months			
Median age at diagnosis (range)	36 (1-265)	31 (11-63)	36 (1-265)
Median age of time of sampling (range)	48 (1-265)	65 (11-132)	48 (1-265)
Outcome			
DOD	11	3	8
NED	11	1	10
AWD	10	2	8
NA	3	0	3
Genomic subgroup[a]			
MNA	6	1	5
MNA + 11q-deleted	2	1	1
11q-deleted	16	2	14
17q-gain	6	1	5
Other structural	5	1	4
Genomic alterations			
TERT or ATRX	18	3	15
ALK-mutation	4	1	3
Cell cycle (CCND1, CDKN2A/B, MDM2 or CDK4)	6	3	3
1p-del	16	1	15
2p-gain	16	5	11
Segmental 17q-gain/wcg17	28/7	6/0	22/7
Number of somatic events			
Median SV (range)	28 (1-89)	33 (28-89)	26 (81-85)
Median SNV (range)	18 (1-81)	24 (8-37)	18 (1-81)

MNA, MYCN-amplified; DOD, dead of disease; NED, no evidence of disease; AWD, alive with disease; wcg, whole chromosome gain; SV, structural variant; SNV, single nucleotide variant. [a]Genomic subgroup given according to Caren *et al* 2010 (7).

in Table SI. Sanger sequencing of amplicons was performed by Eurofins Genomics following standard conditions. The sequencing visualization and analysis was performed using SnapGene viewer software version 5.1 (www.snapgene.com), to verify *LSAMP* rearrangements.

Cell transfection, proliferation, viability and differentiation assays. To evaluate the role of LSAMP in proliferation and viability, *LSAMP* was silenced in the *LSAMP*-expressing cell lines SH-SY5Y and SK-N-BE(2), whereas re-/overexpression of *LSAMP* was conducted in the KELLY and SK-N-AS cell lines (with homozygous and heterozygous *LSAMP* deletion, respectively). Knockdown of *LSAMP* was performed using pre-designed short hairpin (sh)RNA lentiviral particles from Santa Cruz Biotechnology, Inc. *LSAMP* shRNA (h) Lentiviral Particles (cat. no. sc-78206-V) were used and Control shRNA Lentiviral Particles-A (cat. no. sc-108080) were used as the control, whereas copGFP-Control Lentiviral Particles (cat. no. sc-108084) was used for optimization and determination of initial transfection efficiency in parallel experiments. Transduction using lentiviral particles was performed with $1x10^5$ particles and $1x10^5$ cells, corresponding to a multiplicity of infection of 1, in 1 ml medium per well in 12-well plates using Polybrene (cat. no. sc-134220) at a final concentration of 8 μg/ml. After 48 h transduction, the medium containing lentiviral particles and Polybrene was replaced with complete medium lacking Polybrene. Stable cells were selected by adding puromycin (2 μg/ml) to the medium 72 h post-transduction, with changes of fresh medium supplemented with puromycin (2 μg/ml) every 3-4 days during the expansion for further analysis. To re-/overexpress *LSAMP*, pCMV6-AC-LSAMP and pCMV6-AC (control) plasmids (GeneArt; Thermo Fisher Scientific, Inc.) were used. The GFP-tagged constructs pCMV6-AC-LSAMP-GFP and pCMV6-AC-GFP were seeded in parallel experiments in order to determine initial transfection efficiency as well as cellular protein localization. All constructs were verified by Sanger sequencing. The transfection was conducted in

10-cm plates containing $2.5x10^6$ cells/well using 1 μg respective vector dissolved in Lipofectamine® 3000 (Invitrogen; Thermo Fisher Scientific, Inc.). The medium was changed 24 h after transfection and 200 μg/ml neomycin was added 48 h post-transfection for the selection of stable transfects. The medium was replaced with fresh medium supplemented with neomycin (200 μg/ml) every 3-4 days and cells were expanded for further analyses. Real-time measurements of cell proliferation were performed for 96 h using E-plates in the xCELLigence RTCA DP Instrument (Agilent Technologies, Inc.) according to the manufacturer's protocol, which uses impedance for live monitoring of proliferation. By contrast, cell viability was monitored after 72 h of seeding using Presto Blue HS (Thermo Fisher Scientific, Inc.), according to the manufacturer's protocol with a 15-min incubation with the Presto Blue HS reagent prior to absorbance measurement. Each group was assessed four times in 96-well plates and all experiments were repeated three times.

To evaluate the effect of *LSAMP* silencing on differentiation capacity, SK-N-BE(2) and SH-SY-5Y cells were seeded at a density of 750 cells/well in 96-well plates 1 day before replacing the medium with differentiation medium, which consisted of high-glucose medium supplemented with 2.5% FBS and 7.5 μM retinoic acid (RA; MilliporeSigma). High-glucose medium supplemented with 2.5% FBS and 0.075% EtOH was used as a control. The medium was then changed 4 days after seeding and neurite extension was evaluated using a fluorescence microscope after 7 days of RA incubation using a neurite outgrowth staining kit (cat. no. A15001; Thermo Fisher Scientific, Inc.) according to the manufacturer's protocol.

Reverse transcription-quantitative PCR (RT-qPCR). RNA was extracted from 14 NB cell lines and transfected cells (maximum 80% confluence) using RNeasy plus mini kit (Qiagen GmbH), and was quantified spectrophotometrically using a NanoDrop spectrophotometer (NanoDrop; Thermo Fisher Scientific, Inc.). cDNA synthesis was conducted using the Superscript IV VILO master mix according to the manufacturer's protocol (Invitrogen; Thermo Fisher Scientific, Inc.). qPCR was performed using TaqMan™ Fast Advanced Master Mix (Applied Biosystems; Thermo Fisher Scientific) under standard conditions in a 7500 Real-Time PCR system (Applied Biosystems; Thermo Fisher Scientific) under the following conditions: Initial hold at 95˚C for 2 min, followed by 40 cycles of denaturation at 95˚C for 3 sec and annealing/extension at 60˚C for 30 sec. The following probes were used: *LSAMP* pre-designed TaqMan probes covering three different exon boundaries (Exon 1-2; Hs01082649_m1, exon 2-3; Hs01082650_m1 and exon 4-5; Hs01082652_m1; Thermo Fisher Scientific, Inc.) and two housekeeping gene probes, qA-01-0104P5 (*ACTB*) and qA-01-0105P5 (*YWHAC*) (both from TATAA Biocenter AB). The housekeeping genes used, *ACTB* and *YWHAC,* were selected and verified using a human reference gene panel (cat. no. A101) from TATAA Biocenter AB and analyzed by GeneEx (https://bio.tools/geneex). Gene expression analysis was performed using the $2^{-\Delta\Delta Cq}$ method (49).

Kaplan-Meier analysis. Kaplan-Meier analysis with calculation of log-rank test for overall and event-free survival probability in relation to the expression levels of *LSAMP* and other members of the IgLON family (*OPCML, NTM, IGLON5* and *NEGR1*) was performed using the Kaplan-scan cutoff method in 'R2: Genomic Analysis and Visualization Platform' (http://r2.amc.nl) with the publicly available dataset 'Tumor Neuroblastoma-SEQC-498-rpm-Seqnb1' (n=498). The Kaplan-scan cutoff method examines every increasing expression value as cutoff for log-rank test in order to find the optimal segregation point of two groups based on gene expression. This method then presents the most statistically significant cutoff with corresponding Bonferroni corrected P-value together with the initial non-corrected P-value.

Statistical analysis. The proliferation and viability studies were performed on at least three repeats per respective cell line, and included at least four replicates per sample and assay. Cell proliferation was measured every hour during 96 h. Two-way repeated measures (RM) ANOVA was used to determine the significance of the proliferation differences between two groups over time. The Geisser-Greenhouse ε correction was applied following ANOVA, since the experiment includes multiple measurements over time, the sphericity of the sample cannot be assumed. Cell viability was measured 72 h after cell seeding. Unpaired two-sided t-test analysis was performed using the normalized mean value of each assay, to compare the means of two groups, assuming Gaussian distribution. *LSAMP* expression levels in the different NB cell lines were quantified by RT-qPCR in triplicate and qPCR was repeated three times. Differences in *LSAMP* expression in cell lines were analyzed using unpaired two-sided t-test, comparing the means from two groups with different *LSAMP* status (wild type vs. SVs). Comparison of *LSAMP* expression levels in human NB tumors with or without *MYCN* amplification was performed by one-way ANOVA, whereas the correlation of gene expression levels of *LSAMP, OPCML, NTM, IGLON5* and *NEGR1* was assessed using Pearson correlation coefficient analysis, both using the 'Tumor Neuroblastoma-SEQC-498-rpm-Seqnb1' (n=498) dataset (http://r2.amc.nl). All statistical analyses were performed using GraphPad 9.2.0 (GraphPad Software, Inc.). $P<0.05$ was considered to indicate a statistically significant difference.

Results

Copy number analysis detects recurrent focal alterations of LSAMP. Through copy number profiling and structural variation calling from WGS analysis, somatic focal rearrangements located within chromosomal region 3q13.31 were observed at the heterozygous level in tumor tissue from six out of the 35 investigated NB tumor samples (Fig. 1A and B). Analysis of these rearrangements revealed that the breaks were located within or in the vicinity of the *LSAMP* gene (Table II), resulting in disruption of the gene. SNP-microarray performed on the same tumor tissue verified these segmental alterations (Fig. S1A and B), whereas the specific breakpoints in *LSAMP* were verified by PCR and Sanger sequencing (Fig. S2).

From the seven tumors included in our previous study, from which primary and relapsed material was available, *LSAMP* rearrangement was present in two. In these two cases, the rearrangements were present in the relapsed tumors only

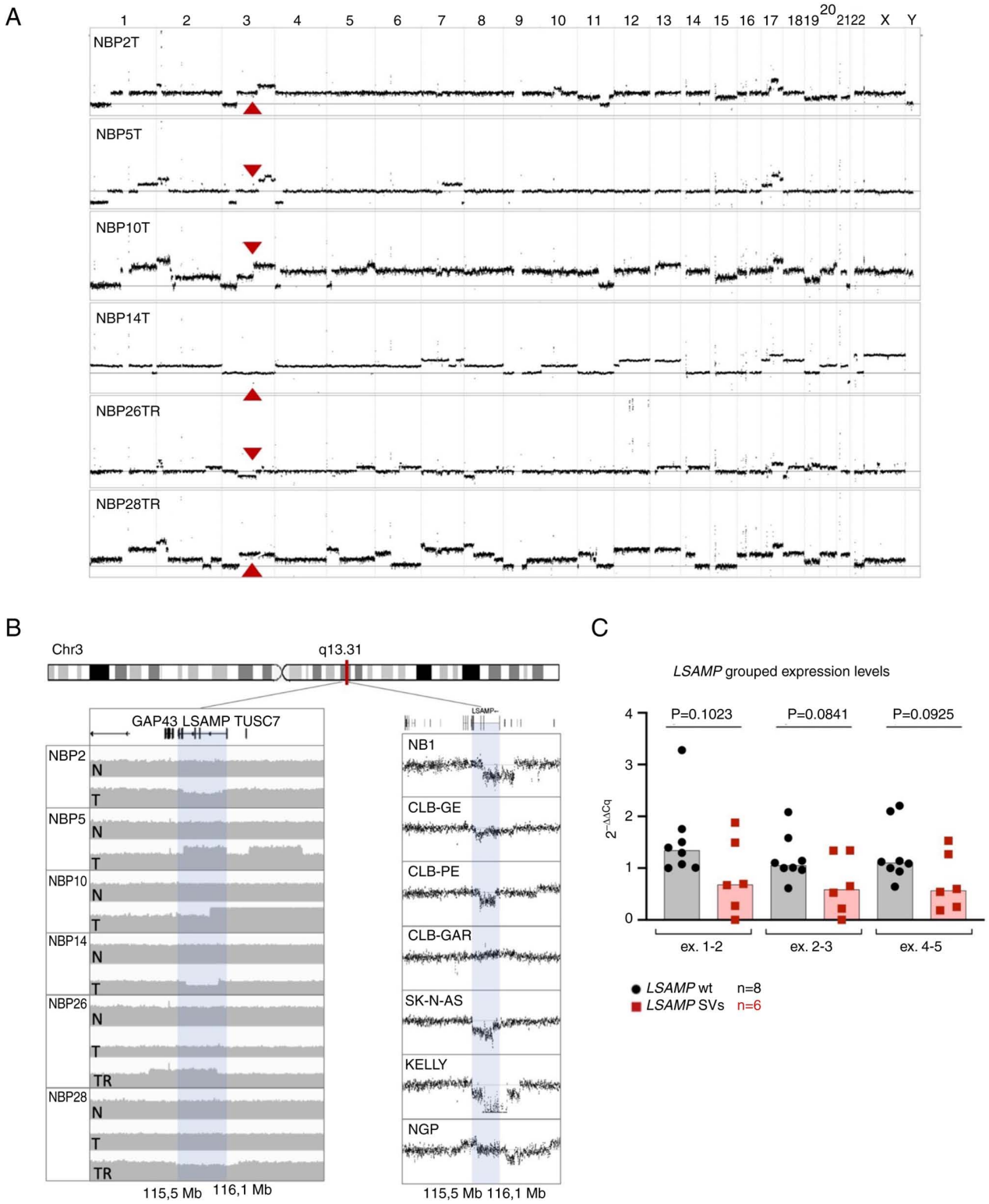

Figure 1. Overview of focal segmental alterations at the 3q13.31 locus. (A) Global chromosome view and copy number calling from WGS for the six NB samples with *LSAMP* rearrangement. The red arrows indicate the 3q13.31 breakpoints. (B) Left panel: WGS-coverage profiles from IGV showing the difference in coverage in the 3q13.31 region connected to segmental alterations. Panels show coverage of N, T and TR samples. Right panel: Single nucleotide polymorphism-microarray profiles of the 3q13.31 locus for the seven different NB cell lines with *LSAMP* rearrangements. (C) *LSAMP* expression levels for three different exon boundaries in NB cell lines in relation to the presence of 3q13.31 rearrangements. The difference in expression levels were analyzed using unpaired two-sided t-test. *LSAMP*, limbic system-associated membrane protein; N, normal; NB, neuroblastoma; SVs, structural variants; T, tumor at time of diagnosis; TR, tumor at time of relapse; WGS, whole genome sequencing; wt, wild type.

and not in the primary tumors (cases NBP26 and NBP28) (10) (Fig. 1B; left panel). WGS did not detect any non-synonymous mutations in *LSAMP* among the investigated tumors.

Other large recurrent segmental or genomic alterations detected in the six NB samples with *LSAMP* rearrangement included 1p/1q-imbalance (n=4), 2p-gain (n=5), 3p-deletion

Table II. Position and type of 3q13.31 alteration.

	3q13.31 alteration		
Case	Type	Position	Other genomic features
NBP2	Deletion	chr3:115.582.490-116.120.525	1p/1q-imbalance, 2p-gain, MNA, 3p-del, 3q-gain, 10q-gain, 11q-del, 17q-gain
NBP5	Deletion	chr3:116.165.059-116.472.978	1p/1q-imbalance, 2p-gain, MNA 3p-del, 3q-gain, 4p-del, 7q-gain, 17q-gain, *TERT* SV, *CDKN2A*-del
NBP10	Translocation	t(1;3)(114.696.299)(115.952.494)	1p/1q-imbalance, 2p-gain, 3p-del, 3q-gain, 4p-del, 5p-del, 5q-gain, 11q-del, 17q-gain, 20q-gain, 21q-del, *ARID1A* SV, *TERT* SV
NBP14	Deletion	chr3:115.624.534-116.061.783	1q-del, interstitial 7q-del, 17q-gain, 21q-del, 22q-gain, *ATRX*-del
NBP26	Tandem duplication	chr3:115.150.006-116.052.713	2p-gain, 2q-gain, interstitial 3q-del, 5q-gain, 6q-gain, 8p-del, 12q-amplification (*CDK4*/*MDM2*), 17q-gain, 18p-del, 19q-gain, interstitial Xp-gain
NBP28	Deletion	chr3:115.505.427-116.344.076	1p/1q-imbalance, 2p-gain, interstitial 2q-del, 3p-del, 5p-gain, 6q-del, 7p-gain, 8p-gain, 9p-del, 11q-del, 14q-del, 17q-gain, *TERT* SV

MNA, *MYCN*-amplified; del, deletion, SV, structural variant.

(n=4), 4p-deletion (n=2), 17q-gain (n=6), 11q-deletion (n=3), *MYCN*-amplification (n=2), and break in proximity of *TERT* or in *ATRX* (n=4) (Fig. 1A; Table II). Major genomic alterations detected in the full cohort are summarized in Table I. In addition to the primary tumor material, 16 NB cell lines were analyzed by SNP-microarrays. This analysis revealed that seven out of the 16 cell lines (NB1, CLB-GE, CLB-PE, CLB-GAR, SK-N-AS, KELLY and NGP) had segmental alterations involving *LSAMP*, including a homozygous deletion within *LSAMP* detected in KELLY (Fig. 1B, right panel; Fig. S1C).

Segmental alterations are associated with a decreased gene expression in NB cell lines. In order to analyze whether the expression levels of *LSAMP* differed between the cell lines with and without segmental alterations, TaqMan probes intersecting three different exon boundaries (exons 1-2, 2-3 and 4-5) were utilized (Fig. S3C). After unpaired two-sided t-test, no statistically significant differences in *LSAMP* expression levels were observed when comparing cell lines with and without 3q13.31 SVs (Figs. 1C and S3A); however, a trend of lower expression was observed in the cell lines with 3q13.31 SVs. Furthermore, in the case of a homozygous deletion break point inside of *LSAMP*, i.e. in the KELLY cell line, no expression was detected at exons 1-2 and 2-3, and very low expression was detected at exon 4-5 (Fig. S3A).

Knockdown of LSAMP restimulates NB cell proliferation in vitro. To investigate the effect of *LSAMP* knockdown on the *LSAMP*-expressing cell lines SH-SY5Y and SK-N-BE(2), shRNA lentiviral particles were used. Initial transduction success for SH-SY5Y and SK-N-BE(2) cells was ~70% for both cell lines, as judged by the number of GPF-expressing cells among control cells transduced with copGFP-Control lentiviral particles (data not shown). Determination of knockdown efficiency through qPCR showed a ~50% reduction in *LSAMP* expression levels in silenced cells as compared with stable cells transduced with control shRNA (Fig. S3B, left panel). After the selection of stable clones, proliferation and viability analyses were conducted. Knockdown of *LSAMP* led to statistically significant increase in proliferation in both SH-SY5Y and SK-N-BE(2) cell lines after 96 h [two-way RM ANOVA with the Geisser-Greenhouse ε correction; SH-SY5Y, $P<0.0001$; SK-N-BE(2), $P=0.045$; Fig. 2A]. A significant difference in viability after 72 h was also seen after *LSAMP* knockdown in SH-SY5Y (unpaired t-test; $P=0.004$) and SK-N-BE(2) (unpaired t-test; $P=0.0004$) cells (Fig. 2C). Knockdown of *LSAMP*, with or without the presence of RA, did not exhibit any major effect on neurite extension in SH-SY5Y and SK-N-BE(2) cells (Fig. S4).

LSAMP re- and overexpression inhibits NB proliferation and viability in vitro. In order to investigate how the re-expression and overexpression of *LSAMP* can affect cell proliferation and viability, KELLY cells (in which *LSAMP* is homozygously deleted) and SK-N-AS cells (which have a heterozygous *LSAMP* deletion) were used, as both display low expression levels of *LSAMP*. Initial transfection efficacy for KELLY and SK-N-AS cells was 70%, as judged by the expression of GFP in cells transfected with pCMV6-AC-GFP at the same occasion (data not shown). Evaluation by qPCR showed a significant increase of *LSAMP* expression levels in *LSAMP*-transfected cells as compared with in pCMV6-AC-tranfected controls (Fig. S3B, right panel). Re- and overexpression of *LSAMP* in KELLY and SK-N-AS cells both led to a significant decrease in cell proliferation after 96 h (two-way RM ANOVA with Geisser-Greenhouse's ε correction; $P<0.0001$; Fig. 2B) as

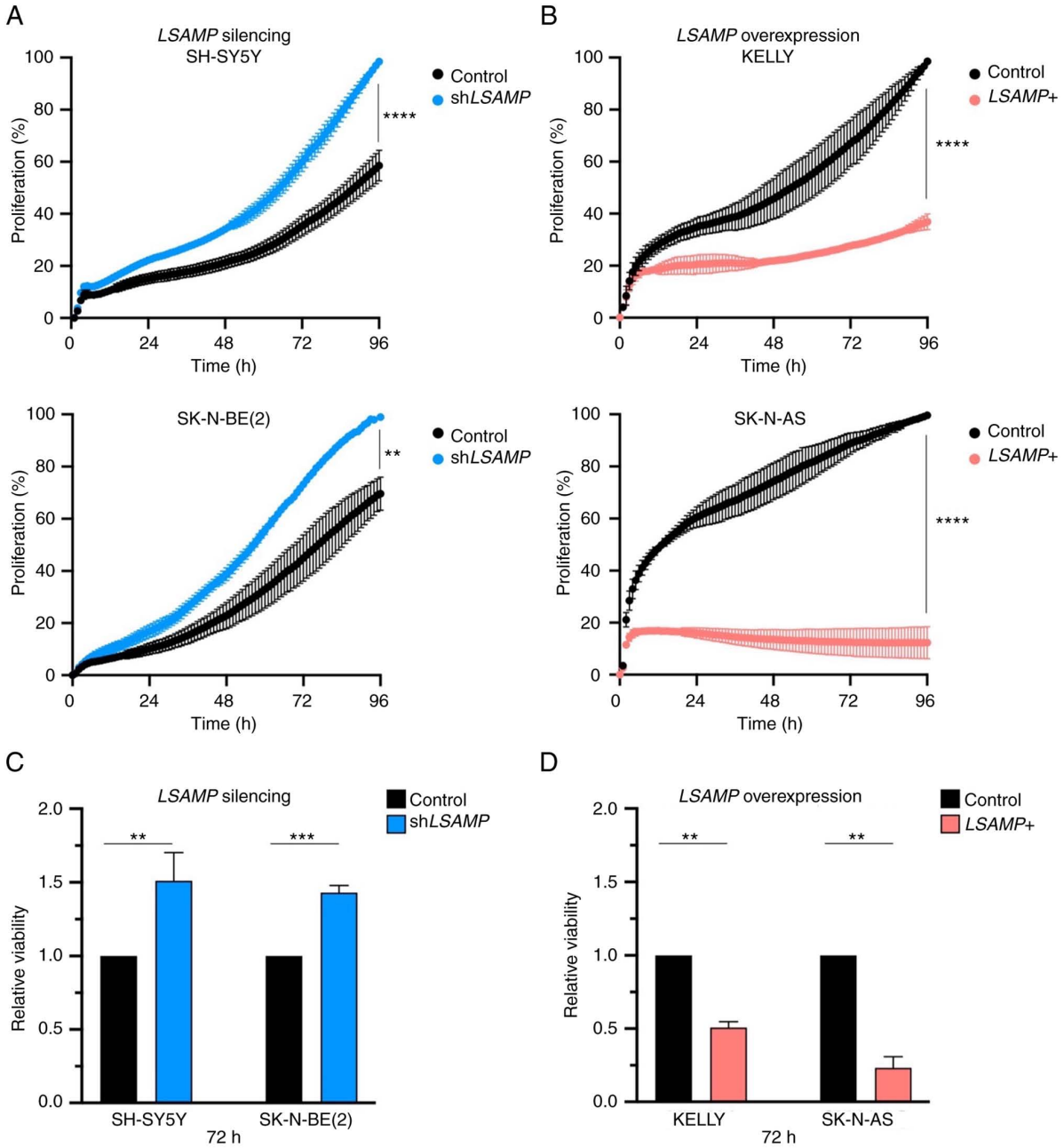

Figure 2. Proliferation and viability after *LSAMP* silencing and overexpression. (A) Real-time monitoring of proliferation after *LSAMP* knockdown for 96 h by xCELLigence in SH-SY5Y and SK-N-BE(2) cells. (B) Real-time monitoring of proliferation after *LSAMP* re/overexpression for 96 h by xCELLigence in KELLY and SK-N-AS cells. (C) Viability of SH-SY5Y and SK-N-BE(2) cells normalized against control at 72 h after *LSAMP* knockdown. (D) Viability of KELLY and SK-N-AS cells at 72 h after *LSAMP* re/overexpression. The significant differences in proliferation were calculated using two-way repeated measures ANOVA, whereas viability was analyzed using two-sided unpaired t-test. *LSAMP*, limbic system-associated membrane protein; sh, short hairpin. **P<0.01, ***P<0.001 and ****P<0.0001.

well as reduced viability after 72 h in KELLY (unpaired t-test; P=0.0022) and SK-N-AS (unpaired t-test; P=0.0032) cells (Fig. 2D). Regarding KELLY cells, viability was also significantly reduced after 96 h (P<0.001; Fig. S3D). Moreover, preliminary data of *LSAMP* overexpression in SH-SY5Y cells also exhibited a significant reduction in viability (data not shown).

Low expression of LSAMP and other members of the IgLON family in patients with NB is associated with poor survival. To investigate the prognostic value of *LSAMP* in NB, the expression levels of *LSAMP* in a publicly available and validated cohort of 498 NB tumors were studied. In this dataset, low *LSAMP* expression was significantly associated with poor patient overall survival and event-free survival (Fig. 3). The association of *LSAMP* with poor overall and event-free survival was most prominent among the non-*MYCN*-amplified cases and to lesser extent among the *MYCN*-amplified cases (Fig. S5A), although no statistically significant difference in expression was seen when comparing *MYCN*-amplified vs. non-*MYCN*-amplified NB (Fig. S5B and C). Similar results were seen for other NB cohorts also publicly available from the R2 genomic analysis and visualization platform (data not shown).

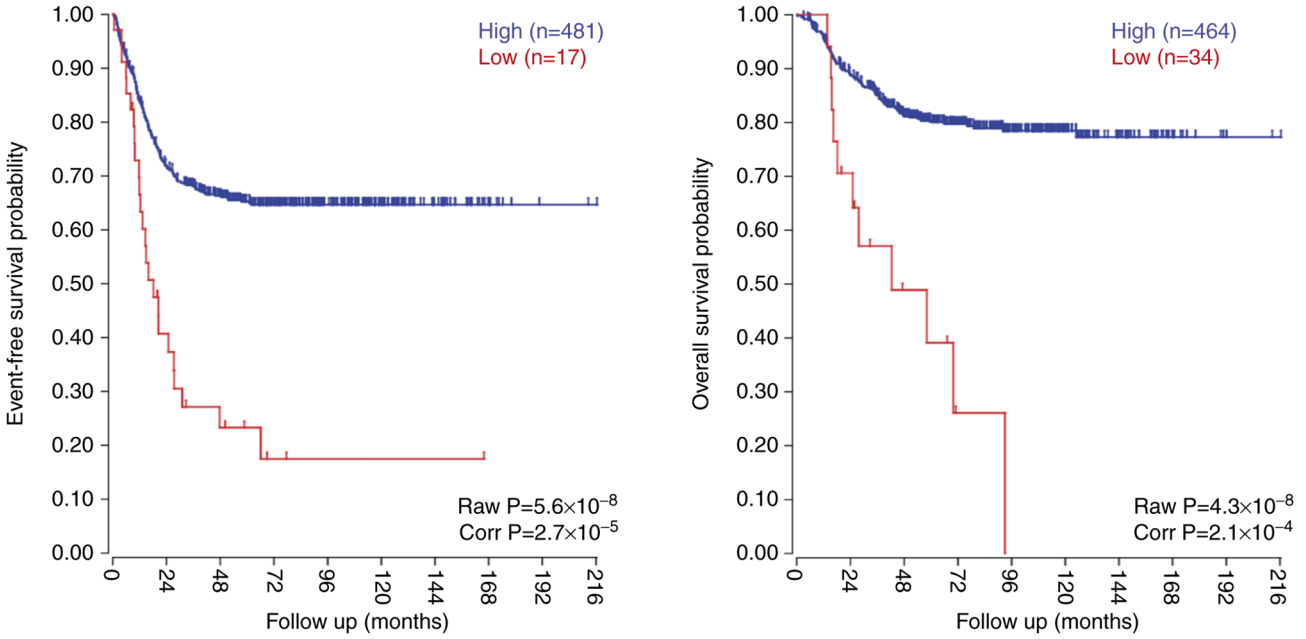

Figure 3. Survival in relation to *LSAMP* gene expression. Low *LSAMP* expression in NB patients was associated with poor overall survival (right panel; adjusted P-value=2.1x10^{-4}) and poor event-free survival (left panel; adjusted P-value=2.7x10^{-5}). Low *LSAMP* expression is indicated in red and high *LSAMP* expression is indicated in blue. *LSAMP*, limbic system-associated membrane protein; Raw, unadjusted P-value; Corr, Bonferroni corrected P-value

Investigation of other members of the IgLON family, *OPCML*, *NTM*, *IGLON5* and *NEGR1*, using the same NB dataset as aforementioned, revealed that low expression of these genes was also significantly associated with poor overall and event-free survival (Fig. S6A). However, no strong correlation in gene expression was detected between any of the different IgLON members (Fig. S6B).

Discussion

By WGS and SNP-microarrays, recurrent focal segmental rearrangements affecting the *LSAMP* gene located at chromosomal region 3q13.31 were detected in six out of 35 NB tumor samples (17%) as well as in seven out of 16 NB cell lines (44%). The *LSAMP* alterations were co-occurring with several other genomic alterations, including *MYCN*-amplification, 1p-deletion, 11q-deletion and 17q-gain, in which the latter was observed in all cases with *LSAMP* aberration. The co-occurrence of 17q-gain indicated that they are a part of a subgroup associated with a worse prognosis. However, segmental and numerical gains affecting the long arm of chromosome 17 is the most common chromosomal aberration in NB present in all genomic subgroups (7), and thus not unique for cases with *LSAMP* alterations. WGS did not detect any pathogenic or likely pathogenic variants in *LSAMP*. However, the genetic etiology with few somatic mutations indicated that NB is mainly driven by genomic events that cause copy number alterations, lead to enhancer hijacking or disruption of genes. Thus, the lack of point mutations in favor of segmental alterations of *LSAMP* is not completely surprising.

LSAMP has a selective role in neuronal growth, which is also interesting from a NB research perspective. In addition, recurrent alterations in other genes associated with neurodevelopment and NB have recently been described by Lopez *et al* (17). Notably, *LSAMP* has previously been described as a tumor suppressor gene in osteosarcoma (33-37), ovarian cancer (38), renal cell carcinoma (39), prostatic cancer (40,41), epithelioid glioblastoma (42), myeloid leukemia (43) and recently in lung cancer (44). Gene expression analysis among NB cell lines indicated that the average expression levels were lower in *LSAMP*-rearranged samples, although no statistically significant difference was detected between the groups; however, in the cell line KELLY with a homozygous deletion rearrangement inside *LSAMP*, no expression levels were detected at exons 1-2 and 2-4. The low expression of *LSAMP* in cell lines lacking the 3q13.31 rearrangement could be due to epigenetic alterations or other mechanisms, as found in lung cancer and clear cell renal cell carcinoma (33,38); however, further studies are needed to clarify this. In order to study the expression and regulation of *LSAMP* in NB, knockdown and re-/overexpression experiments were performed in different NB cell lines. *LSAMP* knockdown led to a significant increase in cell proliferation and viability in the *LSAMP* wild-type cell lines SH-SY5Y and SK-N-BE(2). These results are in concordance with previous publications (33-44), suggesting that *LSAMP* could be a putative tumor suppressor gene also in NB. In addition, re-expression of *LSAMP* in KELLY cells (with homozygous *LSAMP* deletion) and overexpression of *LSAMP* in SK-N-AS cells (with heterozygous *LSAMP* deletion) inhibited cell proliferation and viability. The difference in the level of effect on proliferation between SK-N-AS cells, which had major cell loss, compared with KELLY cells, which had only a decrease in proliferation, could possibly be due to the hetero- and homozygous status of *LSAMP* deletion in the respective cell line. As evaluation of apoptosis was not performed, the current study is restricted as we cannot distinguish between cell death or decreased proliferation as a cause of decreased cell viability.

The present study also revealed that low expression of *LSAMP* was associated with poor overall survival in patients with NB, which supports a possible role in aggressive tumor behavior. This association was most evident for the non-*MYCN*-amplified tumors. In the present cohort of mainly high-risk cases, SVs affecting *LSAMP* were present in different genomic subgroups (*MYCN*-amplified, *MYCN*-amplified together with 11q-deletion, 11q-deleted, 17q-gain and other structural aberrations). A study of a larger cohort reported that SVs affecting *LSAMP* were predominantly found in non-*MYCN*-amplified high-risk tumors (17). However, the higher occurrence of *LSAMP* SVs in cell lines relative to patient tumor samples indicated that this alteration might be a later event contributing to tumor progression rather than initiation. Furthermore, for two of the tumors, *LSAMP* rearrangements were detected in the tumor during relapse, but not at the time of diagnosis. These findings also supported the hypothesis that *LSAMP* alterations are not associated with initial tumor development but rather contribute to the progression of the disease or the promotion of cell migration. No major difference in neurite extension was seen after *LSAMP* knockdown in NB cell lines. However, the current study is limited and additional investigations exploring longer or other differentiation conditions, together with additional cell lines, is required for a better understanding of LSAMP in the context of cell differentiation.

LSAMP is a member of the IgLON family, which is a subgroup of cell adhesion molecules involved in diverse roles in neuronal development (18), and which can also function as tumor suppressor genes (26,50-53). The main members of this family are all located in other chromosomal regions that are frequently deleted in NB and associated with poor prognosis; *NEGR1* is located in 1p31, *IGLON5* is located in 19q13, and *OPCML* and *NTM* are located in 11q25, a chromosomal region that is commonly included in 11q-deleted NB and also in a subset of *MYCN*-amplified NB (7,16,54,55). Notably, low expression of these family members was associated with poor overall and event-free survival, but did not exhibit obvious correlation with *LSAMP* expression levels in NB. In addition, studies in lung cancer have shown that *NEGR1* is involved in the regulation of *LSAMP* and that *LSAMP* can be linked to cancer cell migration through epithelial-mesenchymal transition (44). A similar finding was reported in another study in which depletion of *NEGR1* led to increased cell migration and invasion (53). The presence of *LSAMP* alterations were detected at the heterozygous level in most cases, which would imply haploinsufficiency; however, an additional level of complexity is added from the fact that IgLONs have a conserved interaction mode with the capability of binding to each other as homodimers and heterodimers (56). LSAMP can heterodimerize with either OPCML or NTM, both 11q-localized (57), and if the dimerization partner of LSAMP is not present, this could also possibly affect proper function. This suggests that decreased levels of *LSAMP*, possibly in combination with decreased levels of other IgLON members, may facilitate tumorigenesis through mechanisms affecting proliferation, migration or contact inhibition. However, the specific role of the different IgLON family members in NB pathogenesis is so far speculative and requires further investigation. Furthermore, having in consideration the highly conserved molecular features of IgLONs, it would be interesting to study the possible implications of *LSAMP* downregulation on MAPK/PI3K signaling, as NEGR1 has been reported to be related with this relevant pathway in cancer (18,58).

In conclusion, the present sequencing analyses detected novel recurrent somatic alterations involving *LSAMP*, a cell adhesion molecule that functions in neural crest development and neurite extension. The *in vitro* studies revealed that *LSAMP* may have an anti-proliferative function in NB, possibly through the dysfunction of intercellular adhesion and neural differentiation.

Acknowledgements

Not applicable.

Funding

This work has been supported by grants from the Assar Gabrielsson foundation, the Swedish Childhood Cancer Foundation (grant no. SF: PR2018-099, 15-0061) and the Swedish Research Council (grant no. SF: 521-2014-3031).

Availability of data and materials

The genetic datasets from patients associated with this manuscript are not publicly available due to protection from complete disclosure of genome data according to the consent form. SNP-microarray data generated and/or analyzed during the current study are available in the Gene Expression Omnibus database under accession no. GSE209728 (https://www.ncbi.nlm.nih.gov/geo/query/acc.cgi?acc=GSE209728). Other datasets used and/or analyzed during the current study are available from the corresponding author on reasonable request.

Authors' contributions

AMM conceived and designed experiments. AMM, AD, JG and SF performed the experiments, analyzed and interpreted the data. PK helped with patient care and obtaining clinical information. SF designed the study, formulated strategy and directed the research. AMM and SF confirmed the authenticity of all the raw data and drafted the manuscript. All authors read and approved final version of the manuscript.

Ethics approval and consent to participate

All NB samples from Swedish patients were collected after obtaining written informed consent from their parents or guardians, and were analyzed according to permits approved by the Karolinska Institutet and the Karolinska University Hospital ethics committees (Stockholm, Sweden; approval no. 2009/1369-31/1) in agreement with The Declaration of Helsinki.

Patient consent for publication

Not applicable.

Competing interests

The authors declare that they have no competing interests.

References

1. Diller GP and Baumgartner H: Sudden cardiac death during exercise in patients with congenital heart disease: The exercise paradox and the challenge of appropriate counselling. Eur Heart J 37: 627-629, 2016.
2. Stiller CA and Parkin DM: International variations in the incidence of neuroblastoma. Int J Cancer 52: 538-543, 1992.
3. Park JR, Eggert A and Caron H: Neuroblastoma: Biology, prognosis, and treatment. Hematol Oncol Clin North Am 24: 65-86, 2010.
4. London WB, Castleberry RP, Matthay KK, Look AT, Seeger RC, Shimada H, Thorner P, Brodeur G, Maris JM, Reynolds CP and Cohn SL: Evidence for an age cutoff greater than 365 days for neuroblastoma risk group stratification in the children's oncology group. J Clin Oncol 23: 6459-6465, 2005.
5. Maris JM, Hogarty MD, Bagatell R and Cohn SL: Neuroblastoma. Lancet 369: 2106-2120, 2007.
6. Janoueix-Lerosey I, Schleiermacher G, Michels E, Mosseri V, Ribeiro A, Lequin D, Vermeulen J, Couturier J, Peuchmaur M, Valent A, *et al*: Overall genomic pattern is a predictor of outcome in neuroblastoma. J Clin Oncol 27: 1026-1033, 2009.
7. Caren H, Kryh H, Nethander M, Sjöberg RM, Träger C, Nilsson S, Abrahamsson J, Kogner P and Martinsson T: High-risk neuroblastoma tumors with 11q-deletion display a poor prognostic, chromosome instability phenotype with later onset. Proc Natl Acad Sci USA 107: 4323-4328, 2010.
8. Guimier A, Ferrand S, Pierron G, Couturier J, Janoueix-Lerosey I, Combaret V, Mosseri V, Thebaud E, Gambart M, Plantaz D, *et al*: Clinical characteristics and outcome of patients with neuroblastoma presenting genomic amplification of loci other than MYCN. PLoS One 9: e101990, 2014.
9. Martinez-Monleon A, Oberg HK, Gaarder J, Berbegall AP, Javanmardi N, Djos A, Ussowicz M, Taschner-Mandl S, Ambros IM, Øra I, *et al*: Amplification of CDK4 and MDM2: A detailed study of a high-risk neuroblastoma subgroup. Sci Rep 12: 12420, 2022.
10. Molenaar JJ, Koster J, Ebus ME, van Sluis P, Westerhout EM, de Preter K, Gisselsson D, Øra I, Speleman F, Caron HN and Versteeg R: Copy number defects of G1-cell cycle genes in neuroblastoma are frequent and correlate with high expression of E2F target genes and a poor prognosis. Genes Chromosomes Cancer 51: 10-19, 2012.
11. Ackermann S, Cartolano M, Hero B, Welte A, Kahlert Y, Roderwieser A, Bartenhagen C, Walter E, Gecht J, Kerschke L, *et al*: A mechanistic classification of clinical phenotypes in neuroblastoma. Science 362: 1165-1170, 2018.
12. Fransson S, Martinez-Monleon A, Johansson M, Sjöberg RM, Björklund C, Ljungman G, Ek T, Kogner P and Martinsson T: Whole-genome sequencing of recurrent neuroblastoma reveals somatic mutations that affect key players in cancer progression and telomere maintenance. Sci Rep 10: 22432, 2020.
13. Molenaar JJ, Koster J, Zwijnenburg DA, van Sluis P, Valentijn LJ, van der Ploeg I, Hamdi M, van Nes J, Westerman BA, van Arkel J, *et al*: Sequencing of neuroblastoma identifies chromothripsis and defects in neuritogenesis genes. Nature 483: 589-593, 2012.
14. Chen QR, Bilke S, Wei JS, Whiteford CC, Cenacchi N, Krasnoselsky AL, Greer BT, Son CG, Westermann F, Berthold F, *et al*: cDNA array-CGH profiling identifies genomic alterations specific to stage and MYCN-amplification in neuroblastoma. BMC Genomics 5: 70, 2004.
15. Vandesompele J, Speleman F, Van Roy N, Laureys G, Brinskchmidt C, Christiansen H, Lampert F, Lastowska M, Bown N, Pearson A, *et al*: Multicentre analysis of patterns of DNA gains and losses in 204 neuroblastoma tumors: How many genetic subgroups are there? Med Pediatr Oncol 36: 5-10, 2001.
16. Fransson S, Ostensson M, Djos A, Javanmardi N, Kogner P and Martinsson T: Estimation of copy number aberrations: Comparison of exome sequencing data with SNP microarrays identifies homozygous deletions of 19q13.2 and CIC in neuroblastoma. Int J Oncol 48: 1103-1116, 2016.
17. Lopez G, Conkrite KL, Doepner M, Rathi KS, Modi A, Vaksman Z, Farra LM, Hyson E, Noureddine M, Wei JS, *et al*: Somatic structural variation targets neurodevelopmental genes and identifies SHANK2 as a tumor suppressor in neuroblastoma. Genome Res 30: 1228-1242, 2020.
18. Kubick N, Brosamle D and Mickael ME: Molecular evolution and functional divergence of the IgLON family. Evol Bioinform Online 14: 1176934318775081, 2018.
19. Kimura Y, Katoh A, Kaneko T, Takahama K and Tanaka H: Two members of the IgLON family are expressed in a restricted region of the developing chick brain and neural crest. Dev Growth Differ 43: 257-263, 2001.
20. Pischedda F and Piccoli G: The IgLON family member Negr1 promotes neuronal arborization acting as soluble factor via FGFR2. Front Mol Neurosci 8: 89, 2015.
21. Yamada M, Hashimoto T, Hayashi N, Higuchi M, Murakami A, Nakashima T, Maekawa S and Miyata S: Synaptic adhesion molecule OBCAM; synaptogenesis and dynamic internalization. Brain Res 1165: 5-14, 2007.
22. Hashimoto T, Maekawa S and Miyata S: IgLON cell adhesion molecules regulate synaptogenesis in hippocampal neurons. Cell Biochem Funct 27: 496-498, 2009.
23. Minhas HM, Pescosolido MF, Schwede M, Piasecka J, Gaitanis J, Tantravahi U and Morrow EM: An unbalanced translocation involving loss of 10q26.2 and gain of 11q25 in a pedigree with autism spectrum disorder and cerebellar juvenile pilocytic astrocytoma. Am J Med Genet A 161A: 787-791, 2013.
24. Karis K, Eskla KL, Kaare M, Täht K, Tuusov J, Visnapuu T, Innos J, Jayaram M, Timmusk T, Weickert CS, *et al*: Altered expression profile of IgLON family of neural cell adhesion molecules in the dorsolateral prefrontal cortex of schizophrenic patients. Front Mol Neurosci 11: 8, 2018.
25. Singh K, Jayaram M, Kaare M, Leidmaa E, Jagomäe T, Heinla I, Hickey MA, Kaasik A, Schäfer MK, Innos J, *et al*: Neural cell adhesion molecule Negr1 deficiency in mouse results in structural brain endophenotypes and behavioral deviations related to psychiatric disorders. Sci Rep 9: 5457, 2019.
26. Ntougkos E, Rush R, Scott D, Frankenberg T, Gabra H, Smyth JF and Sellar GC: The IgLON family in epithelial ovarian cancer: Expression profiles and clinicopathologic correlates. Clin Cancer Res 11: 5764-5768, 2005.
27. Xing X, Cai W, Ma S, Wang Y, Shi H, Li M, Jiao J, Yang Y, Liu L, Zhang X and Chen M: Down-regulated expression of OPCML predicts an unfavorable prognosis and promotes disease progression in human gastric cancer. BMC Cancer 17: 268, 2017.
28. Zhang N, Xu J, Wang Y, Heng X, Yang L and Xing X: Loss of opioid binding protein/cell adhesion molecule-like gene expression in gastric cancer. Oncol Lett 15: 9973-9977, 2018.
29. Tomolonis JA, Agarwal S and Shohet JM: Neuroblastoma pathogenesis: Deregulation of embryonic neural crest development. Cell Tissue Res 372: 245-262, 2018.
30. Zhukareva V, Chernevskaya N, Pimenta A, Nowycky M and Levitt P: Limbic system-associated membrane protein (LAMP) induces neurite outgrowth and intracellular Ca2+ increase in primary fetal neurons. Mol Cell Neurosci 10: 43-55, 1997.
31. Sanz RL, Ferraro GB, Girouard MP and Fournier AE: Ectodomain shedding of limbic system-associated membrane protein (LSAMP) by ADAM metallopeptidases promotes neurite outgrowth in DRG neurons. Sci Rep 7: 7961, 2017.
32. Koido K, Traks T, Balotsev R, Eller T, Must A, Koks S, Maron E, Tõru I, Shlik J, Vasar V and Vasar E: Associations between LSAMP gene polymorphisms and major depressive disorder and panic disorder. Transl Psychiatry 2: e152, 2012.
33. Yen CC, Chen WM, Chen TH, York-Kwan WC, Chih-Hsueh PC, Chiou HJ, Hung GY, Wu HTH, Wei CJ, Shiau CY, *et al*: Identification of chromosomal aberrations associated with disease progression and a novel 3q13.31 deletion involving LSAMP gene in osteosarcoma. Int J Oncol 35: 775-788, 2009.
34. Kresse SH, Ohnstad HO, Paulsen EB, Bjerkehagen B, Szuhai K, Serra M, Schaefer KL, Myklebost O and Meza-Zepeda LA: LSAMP, a novel candidate tumor suppressor gene in human osteosarcomas, identified by array comparative genomic hybridization. Genes Chromosomes Cancer 48: 679-693, 2009.
35. Pasic I, Shlien A, Durbin AD, Stavropoulos DJ, Baskin B, Ray PN, Novokmet A and Malkin D: Recurrent focal copy-number changes and loss of heterozygosity implicate two noncoding RNAs and one tumor suppressor gene at chromosome 3q13.31 in osteosarcoma. Cancer Res 70: 160-171, 2010.
36. Baroy T, Kresse SH, Skarn M, Stabell M, Castro R, Lauvrak S, Llombart-Bosch A, Myklebost O and Meza-Zepeda LA: Reexpression of LSAMP inhibits tumor growth in a preclinical osteosarcoma model. Mol Cancer 13: 93, 2014.
37. Smida J, Xu H, Zhang Y, Baumhoer D, Ribi S, Kovac M, von Luettichau I, Bielack S, O'Leary VB, Leib-Mösch C, *et al*: Genome-wide analysis of somatic copy number alterations and chromosomal breakages in osteosarcoma. Int J Cancer 141: 816-828, 2017.

38. Zhang L, Yuan Y, Lu KH and Zhang L: Identification of recurrent focal copy number variations and their putative targeted driver genes in ovarian cancer. BMC Bioinformatics 17: 222, 2016.
39. Chen J, Lui WO, Vos MD, Clark GJ, Takahashi M, Schoumans J, Khoo SK, Petillo D, Lavery T, Sugimura J, *et al*: The t(1;3) breakpoint-spanning genes LSAMP and NORE1 are involved in clear cell renal cell carcinomas. Cancer Cell 4: 405-413, 2003.
40. Petrovics G, Li H, Stumpel T, Tan SH, Young D, Katta S, Li Q, Ying K, Klocke B, Ravindranath L, *et al*: A novel genomic alteration of LSAMP associates with aggressive prostate cancer in African American men. EBioMedicine 2: 1957-1964, 2015.
41. Huang SP, Lin VC, Lee YC, Yu CC, Huang CY, Chang TY, Lee HZ, Juang SH, Lu TL and Bao BY: Genetic variants in nuclear factor-kappa B binding sites are associated with clinical outcomes in prostate cancer patients. Eur J Cancer 49: 3729-3737, 2013.
42. Nobusawa S, Hirato J, Kurihara H, Ogawa A, Okura N, Nagaishi M, Ikota H, Yokoo H and Nakazato Y: Intratumoral heterogeneity of genomic imbalance in a case of epithelioid glioblastoma with BRAF V600E mutation. Brain Pathol 24: 239-246, 2014.
43. Yoon J, Cho EH, Yun JW, Kim HY, Jang JH, Kim HJ and Kim SH: LSAMP rearrangement in acute myeloid leukemia with a jumping translocation involving 3q13.31. Ann Lab Med 41: 342-345, 2021.
44. Chang CY, Wu KL, Chang YY, Liu YW, Huang YC, Jian SF, Lin YS, Tsai PH, Hung JY, Tsai YM and Hsu YL: The downregulation of LSAMP expression promotes lung cancer progression and is associated with poor survival prognosis. J Pers Med 11: 578, 2021.
45. Roller E, Ivakhno S, Lee S, Royce T and Tanner S: Canvas: Versatile and scalable detection of copy number variants. Bioinformatics 32: 2375-2377, 2016.
46. Chen X, Schulz-Trieglaff O, Shaw R, Barnes B, Schlesinger F, Källberg M, Cox AJ, Kruglyak S and Saunders CT: Manta: Rapid detection of structural variants and indels for germline and cancer sequencing applications. Bioinformatics 32: 1220-1222, 2016.
47. Thorvaldsdottir H, Robinson JT and Mesirov JP: Integrative genomics viewer (IGV): High-performance genomics data visualization and exploration. Brief Bioinform 14: 178-192, 2013.
48. Umapathy G, Guan J, Gustafsson DE, Javanmardi N, Cervantes-Madrid D, Djos A, Martinsson T, Palmer RH and Hallberg B: MEK inhibitor trametinib does not prevent the growth of anaplastic lymphoma kinase (ALK)-addicted neuroblastomas. Sci Signal 10: eaam7550, 2017.
49. Livak KJ and Schmittgen TD: Analysis of relative gene expression data using real-time quantitative PCR and the 2(-Delta Delta C(T)) method. Methods 25: 402-408, 2001.
50. Sellar GC, Watt KP, Rabiasz GJ, Stronach EA, Li L, Miller EP, Massie CE, Miller J, Contreras-Moreira B, Scott D, *et al*: OPCML at 11q25 is epigenetically inactivated and has tumor-suppressor function in epithelial ovarian cancer. Nat Genet 34: 337-343, 2003.
51. Reed JE, Dunn JR, du Plessis DG, Shaw EJ, Reeves P, Gee AL, Warnke PC, Sellar GC, Moss DJ and Walker C: Expression of cellular adhesion molecule 'OPCML' is down-regulated in gliomas and other brain tumours. Neuropathol Appl Neurobiol 33: 77-85, 2007.
52. Cui Y, Ying Y, van Hasselt A, Ng KM, Yu J, Zhang Q, Jin J, Liu D, Rhim JS, Rha SY, *et al*: OPCML is a broad tumor suppressor for multiple carcinomas and lymphomas with frequently epigenetic inactivation. PLoS One 3: e2990, 2008.
53. Kim H, Hwang JS, Lee B, Hong J and Lee S: Newly identified cancer-associated role of human neuronal growth regulator 1 (NEGR1). J Cancer 5: 598-608, 2014.
54. Abbasi MR, Rifatbegovic F, Brunner C, Mann G, Ziegler A, Pötschger U, Crazzolara R, Ussowicz M, Benesch M, Ebetsberger-Dachs G, *et al*: Impact of disseminated neuroblastoma cells on the identification of the relapse-seeding clone. Clin Cancer Res 23: 4224-4232, 2017.
55. Caron H: Allelic loss of chromosome 1 and additional chromosome 17 material are both unfavourable prognostic markers in neuroblastoma. Med Pediatr Oncol 24: 215-221, 1995.
56. Venkannagari H, Kasper JM, Misra A, Rush SA, Fan S, Lee H, Sun H, Seshadrinathan S, Machius M, Hommel JD and Rudenko G: Highly conserved molecular features in IgLONs contrast their distinct structural and biological outcomes. J Mol Biol 432: 5287-5303, 2020.
57. Reed J, McNamee C, Rackstraw S, Jenkins J and Moss D: Diglons are heterodimeric proteins composed of IgLON subunits, and Diglon-CO inhibits neurite outgrowth from cerebellar granule cells. J Cell Sci 117: 3961-3973, 2004.
58. Szczurkowska J, Pischedda F, Pinto B, Managò F, Haas CA, Summa M, Bertorelli R, Papaleo F, Schäfer MK, Piccoli G and Cancedda L: NEGR1 and FGFR2 cooperatively regulate cortical development and core behaviours related to autism disorders in mice. Brain 141: 2772-2794, 2018.